
The following resources related to this article are available online at <http://stke.sciencemag.org>. This information is current as of 31 March 2010.

- Article Tools** Visit the online version of this article to access the personalization and article tools:
<http://stke.sciencemag.org/cgi/content/full/sigtrans;3/115/ra24>
- Supplemental Materials** "*Supplementary Materials*"
<http://stke.sciencemag.org/cgi/content/full/sigtrans;3/115/ra24/DC1>
- References** This article cites 58 articles, 20 of which can be accessed for free:
<http://stke.sciencemag.org/cgi/content/full/sigtrans;3/115/ra24#otherarticles>
- Glossary** Look up definitions for abbreviations and terms found in this article:
<http://stke.sciencemag.org/glossary/>
- Permissions** Obtain information about reproducing this article:
<http://www.sciencemag.org/about/permissions.dtl>

Differential Redox Regulation of ORAI Ion Channels: A Mechanism to Tune Cellular Calcium Signaling

Ivan Bogeski,^{1*} Carsten Kummerow,^{1†} Dalia Al-Ansary,^{1†} Eva C. Schwarz,¹ Richard Koehler,¹ Daisuke Kozai,² Nobuaki Takahashi,² Christine Peinelt,¹ Desiree Griesemer,^{1‡} Monika Bozem,¹ Yasuo Mori,² Markus Hoth,¹ Barbara A. Niemeyer^{1*}

(Published 30 March 2010; Volume 3 Issue 115 ra24)

Reactive oxygen species (ROS) are involved in many physiological and pathophysiological cellular processes. We used lymphocytes, which are exposed to highly oxidizing environments during inflammation, to study the influence of ROS on cellular function. Calcium ion (Ca^{2+}) influx through Ca^{2+} release-activated Ca^{2+} (CRAC) channels composed of proteins of the ORAI family is essential for the activation, proliferation, and differentiation of T lymphocytes, but whether and how ROS affect ORAI channel function have been unclear. Here, we combined Ca^{2+} imaging, patch-clamp recordings and measurements of cell proliferation and cytokine secretion to determine the effects of hydrogen peroxide (H_2O_2) on ORAI channel activity and human T helper lymphocyte (T_H cell) function. ORAI1, but not ORAI3, channels were inhibited by oxidation by H_2O_2 . The differential redox sensitivity of ORAI1 and ORAI3 channels depended mainly on an extracellularly located reactive cysteine, which is absent in ORAI3. T_H cells became progressively less redox-sensitive after differentiation into effector cells, a shift that would allow them to proliferate, differentiate, and secrete cytokines in oxidizing environments. The decreased redox sensitivity of effector T_H cells correlated with increased expression of *Orai3* and increased abundance of several cytosolic anti-oxidants. Knockdown of ORAI3 with small-interfering RNA rendered effector T_H cells more redox-sensitive. The differential expression of *Orai* isoforms between naïve and effector T_H cells may tune cellular responses under oxidative stress.

INTRODUCTION

Intracellular Ca^{2+} is a second messenger involved in the regulation of a diverse range of functions (1). One of the major Ca^{2+} entry pathways into nonexcitable cells, such as lymphocytes and epithelial cells, is through ubiquitously expressed Ca^{2+} release-activated Ca^{2+} (CRAC) channels that are localized in the plasma membrane. Ca^{2+} influx through CRAC channels is activated when inositol 1,4,5-trisphosphate (IP_3) triggers Ca^{2+} release from intracellular stores in the lumen of the endoplasmic reticulum (ER) (2–4). The concomitant decrease in ER luminal Ca^{2+} triggers accumulation of the ER Ca^{2+} sensor protein stromal interaction molecule (STIM1) into puncta close to the plasma membrane (5, 6). These clustered STIM1 proteins directly activate Ca^{2+} influx through CRAC channels, which are encoded by the *Orai* gene family (7–11). ORAI proteins contain four transmembrane domains with both N- and C-terminal intracellular domains (12, 13) that contain putative N-terminal calmodulin-binding domains and C-terminal coiled-coil motifs. *Orai* family members are highly homologous, and *Orai1* and 3 are widely expressed at the messenger RNA (mRNA) level, with *Orai2* showing a somewhat more restricted expression pattern (14, 15). ORAI1 proteins contain the longest

intracellular N termini with two proline-rich regions and one arginine-rich region and a glycosylation site in the extracellular loop between transmembrane regions 3 and 4 (15). Neither ORAI2 nor ORAI3 contain extracellular glycosylation motifs, although ORAI3 displays the longest second extracellular loop (16). In T cells and many other cell types, CRAC channels are mainly formed by ORAI1 (7), although heteromeric channels can assemble with ORAI2 or ORAI3 (15, 17, 18).

Reactive oxygen species (ROS) are important mediators of many physiological and pathophysiological processes (19, 20). They are generated in both the intracellular and the extracellular space by redox-active proteins such as members of the mitochondrial electron transfer chain and NADPH oxidase (nicotinamide adenine dinucleotide phosphate-(NADPH) oxidase) (19, 21, 22). Antioxidants clear ROS and preserve the physiological redox state of cells (19, 23). Of the more than 20 types of ROS, superoxide radicals ($\text{O}_2^{\cdot-}$) and hydrogen peroxide (H_2O_2) appear to be the most biologically relevant (19). H_2O_2 is relatively stable and can diffuse across the cell membrane. It primarily acts by oxidizing cysteine residues in target proteins (19). Physiological H_2O_2 concentrations are difficult to determine and can vary from the nanomolar to the low micromolar range (24–27). The existence of so-called ROS microdomains may even yield a higher local H_2O_2 concentration (28, 29).

Immune cells are exposed to highly oxidizing environments during inflammation (19, 30). Besides having microbicidal effects during the oxidative burst of phagocytes, H_2O_2 can also act as an intracellular second messenger regulating various signaling pathways (19, 20, 30) and may be involved in lymphocyte activation (30). It has also recently been proposed to act as a chemotactic and paracrine signal for leukocyte migration in zebrafish (26).

¹Department of Biophysics, Saarland University, 66421 Homburg, Germany. ²Department of Synthetic Chemistry and Biological Chemistry, Kyoto University, Kyoto 615-8510, Japan.

*To whom correspondence should be addressed. E-mail: ivan.bogeski@uks.eu (I.B.); barbara.niemeyer@uks.eu (B.A.N.)

†These authors contributed equally to this work.

‡Present address: Department of Biology, Technische Universität Kaiserslautern, 67663 Kaiserslautern, Germany.

However, it is not clear whether ROS affect the cellular Ca^{2+} signaling pathways important for lymphocyte function, in particular, if and how CRAC channels are modulated by oxidation.

RESULTS

ORAI1 channels are inhibited by H_2O_2

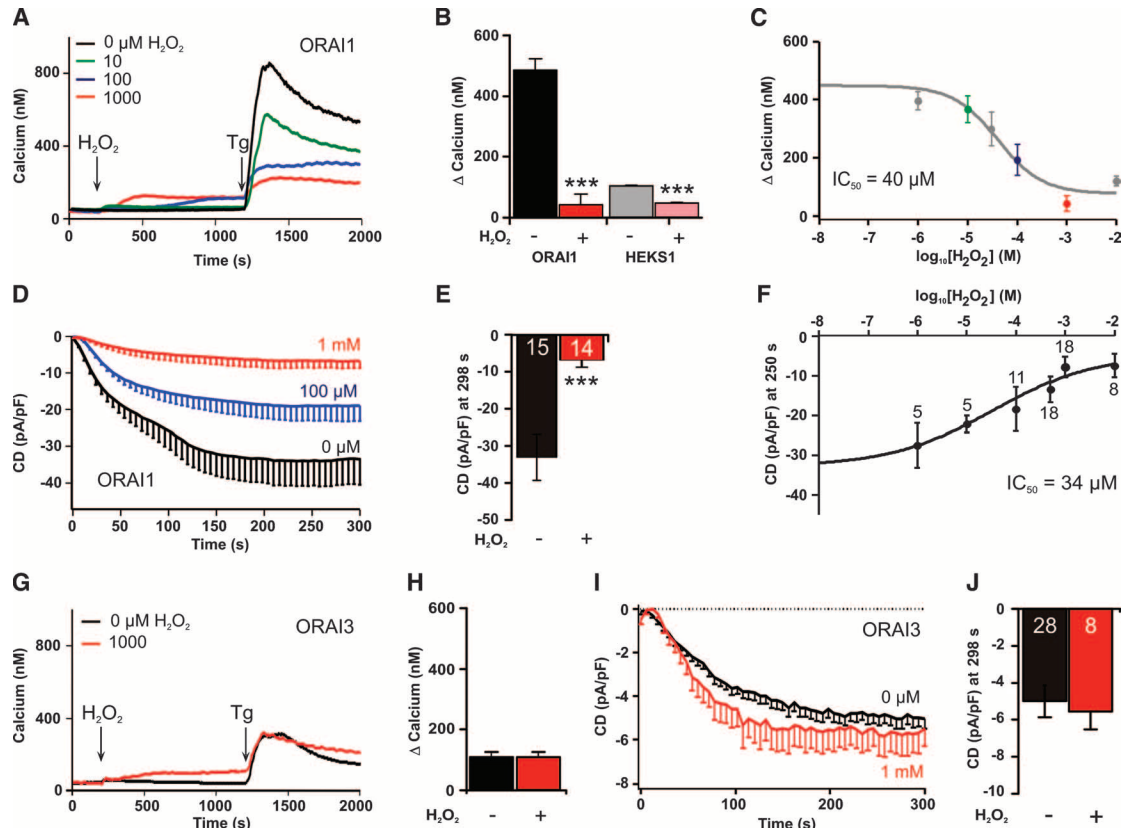
To test whether ORAI1 channels are molecular targets of oxidation, we analyzed the effect of ROS (H_2O_2) on intracellular Ca^{2+} concentrations ($[Ca^{2+}]_i$) and current densities (CDs) of transiently expressed ORAI1 channels in human embryonic kidney (HEK) 293 cells with stable expression of STIM1 (31), referred to as HEKS101 cells. As expected, depletion of internal ER Ca^{2+} stores by thapsigargin (Tg), an inhibitor of the sarco-endoplasmic reticulum Ca^{2+} adenosine triphosphatase (SERCA), induced a large sustained increase of $[Ca^{2+}]_i$ in HEKS101 cells, which was about five times larger than that in HEK293 cells expressing STIM1 alone (HEKS1) (black trace in Fig. 1, A and B). Previous addition of H_2O_2 led to an initial increase in $[Ca^{2+}]_i$ at higher concentrations (see below) and to a subsequent inhibition of the Tg-induced increase in $[Ca^{2+}]_i$ with a median inhibitory concentration (IC_{50}) of 40 μ M (Fig. 1, A to C). To test the effect of H_2O_2 on ORAI1 channels more directly and to exclude effects of H_2O_2 on the membrane potential or Ca^{2+} export, we performed patch-clamp analyses of HEKS101 cells and triggered ORAI1 currents by depletion of ER Ca^{2+} store with IP_3 . This induced inward currents with an average CD of -33 ± 6 pA/pF (Fig. 1, D and E) com-

pared to -0.5 ± 0.1 pA/pF for HEKS1 cells at -80 mV after 5 min. Preincubation with 1 mM H_2O_2 for 10 to 20 min reduced the ORAI1 current size to -6.8 ± 1.9 pA/pF (Fig. 1, D and E). When tested against a range of different H_2O_2 concentrations, CDs decreased with an IC_{50} of 34 μ M (Fig. 1F). Increasing H_2O_2 concentrations also caused a slowing of current activation (Fig. 1D). Addition of H_2O_2 after Tg in HEKS101 cells, Jurkat T cells, and human effector T_H cells neither decreased $[Ca^{2+}]_i$ (fig. S1, A to C) nor blocked I_{CRAC} (fig. S1, D to F). This suggests that oxidation may prevent activation of ORAI channels. To test whether oxidation prevents activation of ORAI channels directly or affects proteins involved in activation that would also activate homologous channels, we investigated the effects of H_2O_2 on ORAI2 and ORAI3 expressed in HEKS1 cells. HEKS102 cells showed similar Ca^{2+} signals and inhibition by H_2O_2 (fig. S2, A and B). HEKS103 cells showed a smaller increase in $[Ca^{2+}]_i$ upon Tg stimulation compared to HEKS101, which was not decreased even by 1 mM H_2O_2 (Fig. 1, G and H). Average CDs of ORAI3 were also smaller when compared to those of ORAI1 but still ~ 10 times larger than in HEKS1 cells (-4.9 ± 0.4 , -33 ± 6 , and -0.5 ± 0.1 pA/pF, respectively; $P < 0.001$). ORAI3 currents, however, were not blocked after preincubation with 1 mM H_2O_2 (Fig. 1, I and J), suggesting that the inhibitory effect of H_2O_2 is specific for ORAI1 channels.

A cysteine residue in ORAI1 is involved in redox sensing

Free thiol groups of cysteine residues are the major targets of oxidation in proteins. Therefore, we compared the number and location of cysteine

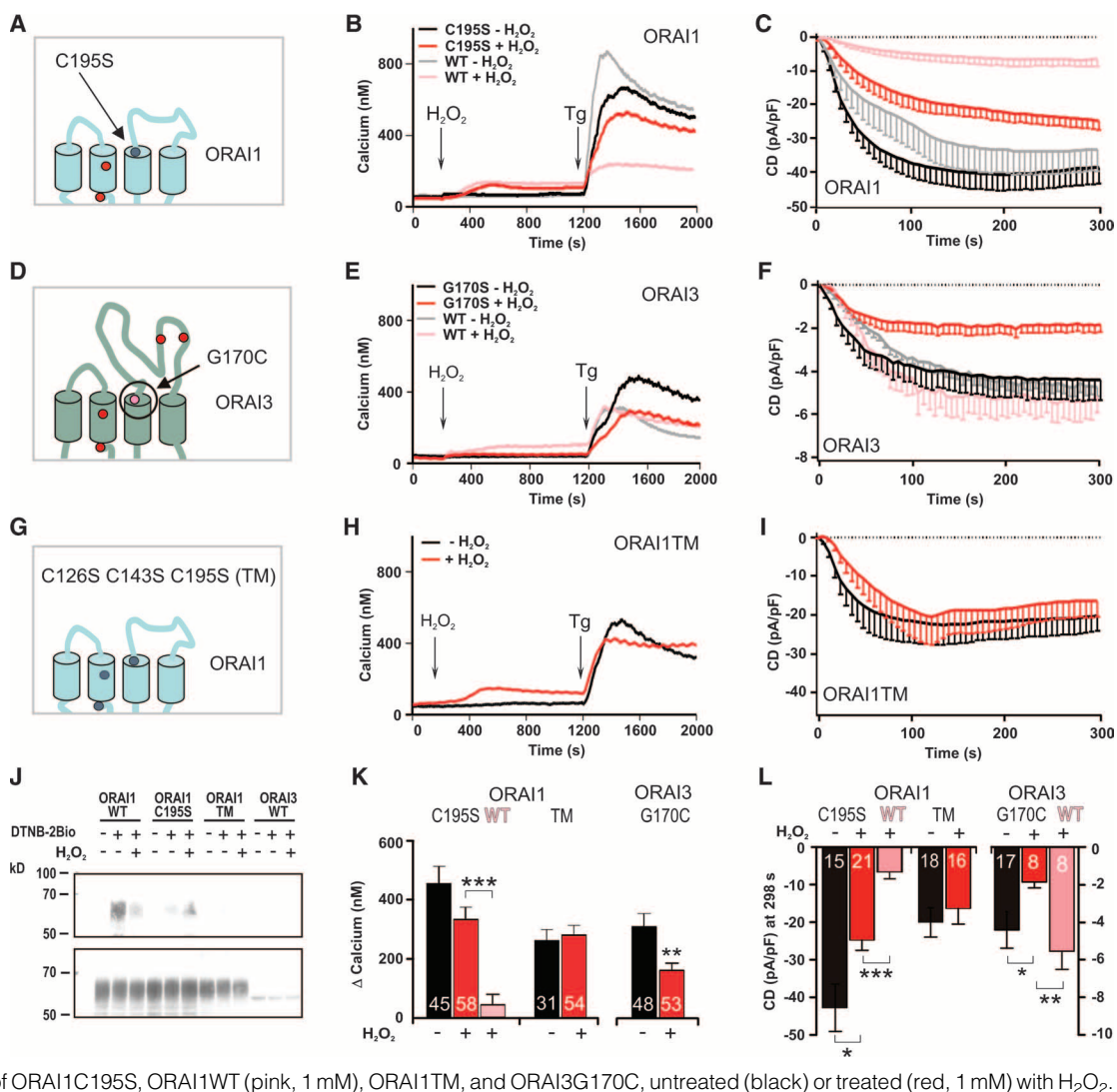
Fig. 1. ORAI1 but not ORAI3 channels are inhibited by H_2O_2 . (A) $[Ca^{2+}]_i$ in HEKS101 cells before and after addition of Tg and without H_2O_2 (black trace, $n = 81$) or with prior addition of different concentrations of H_2O_2 ; green, 10 μ M ($n = 94$); blue, 100 μ M ($n = 71$); red, 1 mM H_2O_2 , ($n = 61$). (B) Tg-induced $\Delta[Ca^{2+}]_i$ between 1200 and 2000 s after treatment with 1 mM H_2O_2 (red and pink, $n = 244$) or without H_2O_2 (black and gray, $n = 244$) in HEKS101 (ORAI1) and HEKS1 cells. (C) Plot of $\Delta[Ca^{2+}]_i$ against $[H_2O_2]$ in HEKS101 cells. (D) CDs without and with 100 μ M or 1 mM H_2O_2 in HEKS101 cells. (E) Average CD in the absence (black) or with 1 mM H_2O_2 (red). (F) Plot of CD against $[H_2O_2]$ in HEKS101 cells. (G) $[Ca^{2+}]_i$ in HEKS103 cells untreated (black, $n = 53$) or treated with 1 mM H_2O_2 (red, $n = 54$). (H) $\Delta[Ca^{2+}]_i$ between 1200 and 2000 s after treatment with 1 mM H_2O_2 (red) or without H_2O_2 (black) in HEKS103 cells. (I) CD of HEKS103 cells plotted versus time; black (untreated), red (1 mM H_2O_2). (J) Average CD with (red) or without H_2O_2 (black). *** $P < 0.001$ (unpaired Student's t test). Error bars indicate means \pm SEM.



residues within the ORAI1 and ORAI3 proteins. ORAI1 contains three cysteines at amino acid positions 126, 143, and 195 (Fig. 2A). ORAI3 also contains cysteine residues at the first two homologous positions, but lacks the homolog of Cys¹⁹⁵. ORAI3 also contains two additional closely spaced cysteines within the extracellular loop between transmembrane regions S3 and S4 (Fig. 2D) that are likely to form a disulfide bond. To detect reactive cysteines in ORAI1 and ORAI3, we incubated permeabilized HEK cells transfected with the relevant green fluorescent protein (GFP)-tagged ORAI protein with DTNB-2Biotin (DTNB-2Bio), which reacts with free thiol groups and can be purified by avidin-based affinity purification. Free thiol groups that can be blocked by pretreatment with H₂O₂ were detected in ORAI1, whereas no overt retention was detected for ORAI3 (Fig. 2J). Although ORAI3 protein input is lower, this finding suggests that Cys¹⁹⁵ may be a possible redox sensor of ORAI1 (Fig. 2J). Mutation of Cys¹⁹⁵ to serine (C195S; see Fig. 2A) significantly reduced the block of Tg-induced increase in [Ca²⁺]_i by 1 mM H₂O₂ relative to that of wild-type ORAI1 (Fig. 2, B and K). Consistently, the H₂O₂-induced current inhibition was significantly smaller for C195S than for the wild

type (Fig. 2, C and L). Although some current inhibition remained, Cys¹⁹⁵ appears to be a major reactive cysteine conferring oxidation-induced reduction of channel activity. To further test the significance of Cys¹⁹⁵, we created a potential gain-of-function mutation in *Orai3* by exchanging the homolog of Cys¹⁹⁵, namely, Gly¹⁷⁰, with cysteine (G170C; Fig. 2D and fig. S2C). As seen from both Ca²⁺ imaging data (Fig. 2, E and K) and patch-clamp analyses (Fig. 2, F and L), introducing the G170C mutation bestowed redox sensitivity on ORAI3, suggesting that Cys¹⁹⁵ is an important redox sensor in ORAI1. Because some current inhibition remained in the ORAI1 C195S mutant, we also mutated the remaining two cysteine residues of ORAI1 (Fig. 2G). The ORAI1 triple mutant (TM, C195S-C143S-C126S) had reduced Ca²⁺ signals relative to those of the wild type, which were not inhibited by H₂O₂ (Fig. 2, H and K). The triple mutant currents were slightly reduced relative to those of the wild type (-20 ± 3.9 pA/pF, $P = 0.08$) but again showed a complete loss of redox sensitivity (Fig. 2, I and L). In parallel to the electrophysiological analyses of the mutants, we also investigated their reactive cysteine content by incorporation of DTNB-2Bio. ORAI1C195S incorporated less DTNB-

Fig. 2. Identification of Cys¹⁹⁵



* $P < 0.05$, ** $P < 0.01$, *** $P < 0.001$, unpaired Student's *t* test.

2Bio than ORAI1 wild type, whereas no incorporation was detected in the triple mutant of ORAI1 or ORAI3 (Fig. 2J). That the triple cysteine ORAI1 mutant still formed functional channels unaffected by high concentrations of H₂O₂ argues against a major role for cysteines in subunit assembly and against redox regulation of components involved in ORAI1 activation (i.e., STIM1) as the cause for reduced currents. None of the mutants showed a gross alteration of the current-voltage relationship, indicating no major alteration of the selectivity filter (fig. S2, D and G).

Redox regulation of Ca²⁺ homeostasis in human T helper cells depends on their differentiation status

Upon migration to sites of inflammation, effector T helper (T_H) cells need to function with an optimal and appropriate response despite highly oxidizing environments. To investigate the physiological importance of redox regulation of ORAI channels, we investigated the effects of H₂O₂ on [Ca²⁺]_i both in naïve CD4⁺ T_H cells that have never been exposed to antigen and in differentiated effector human CD4⁺ T_H cells. To induce effector status, naïve T_H cells isolated from human blood were stimulated with beads coated with antibodies against CD3 and CD28 (32). Similar to the HEKS101 cells, T_H cells responded to an acute application of H₂O₂ with an increase in [Ca²⁺]_i in a concentration-dependent manner (fig. S3, A and B). Naïve T_H cells responded with an apparent median effective concentration (EC₅₀) of ~130 μM and were more sensitive than effector T_H cells that responded with an apparent EC₅₀ of ~740 μM (fig. S3C). This initial Ca²⁺ increase was not due to CRAC channel activation because it was not inhibited by 100 μM of the CRAC channel inhibitor, 2-aminoethoxydiphenyl borate (2-APB) (fig. S3D). The rate of the initial Ca²⁺ increase was inhibited by flufenamic acid (FFA), which interferes with nonselective cation channels (fig. S3D) (33). Patch-clamp analyses of Jurkat T cells revealed an H₂O₂ (1 mM)-induced activation of a nonselective, outwardly rectifying conductance, which was blocked by FFA (fig. S3, E to G). These findings are in agreement with reports that transient receptor potential cation channel subfamily M (TRPM) channels are expressed in human T cells (34, 35) and are activated by H₂O₂ (36, 37). In summary, the H₂O₂-induced Ca²⁺ influx is not mediated by CRAC channels but by nonselective cation channels.

The H₂O₂ sensitivity of ORAI1 channels predicts that store-operated Ca²⁺ signals in T_H cells should be inhibited by H₂O₂. We tested this prediction and found that the Tg-induced increase in [Ca²⁺]_i in naïve and effector T_H cells is dose-dependently inhibited by preincubation with H₂O₂. To analyze this effect independently of the initial [Ca²⁺]_i rise induced by H₂O₂ (fig. S3), we compared the Tg-induced increase in [Ca²⁺]_i in “iso-cells,” that is, in cells with comparable [Ca²⁺]_i (30 to 80 nM) in the presence of 10 μM H₂O₂ before addition of Tg. Following Tg activation, a significant reduction in [Ca²⁺]_i was observed in naïve T_H cells, whereas effector T_H cells were much less sensitive (Fig. 3, A and C). We then analyzed Δ[Ca²⁺]_i in the absence and presence of different H₂O₂ concen-

trations and obtained IC₅₀ values of 7 μM for naïve T_H cells versus 51 μM for effector T_H cells (Fig. 3D). To investigate the differential H₂O₂ effect independently of changes in membrane potential, we performed voltage-clamp experiments. Recordings of I_{CRAC} in naïve T_H cells revealed extremely small currents barely distinguishable from leak currents. We therefore used Jurkat T cells, in which Ca²⁺ imaging responses toward H₂O₂ are similar to naïve T_H cells (fig. S3H). I_{CRAC} was inhibited by 87% in the presence of 500 μM H₂O₂ (Fig. 3, E and F). I_{CRAC} of effector T_H cells, however, showed a reduced sensitivity toward H₂O₂ with only ~40% inhibition (Fig. 3F). Thus, CRAC channels in T_H effector cells are less susceptible toward H₂O₂ than those in naïve T_H cells.

Viability and interleukin-2 (IL-2) secretion are regulated by ROS in a T_H cell differentiation-dependent manner

Changes in intracellular Ca²⁺ signaling regulate activation, differentiation, and proliferation of T cells. Thus, we investigated the effects of H₂O₂ on naïve and effector T_H cell viability and cytokine production. H₂O₂ (100 μM) was added to the medium of T_H cells at different time points after contact with beads coated with antibodies against CD3 and CD28 triggered induction of effector status, and viability was measured 24 hours later (see Materials and Methods for details). Although 100 μM H₂O₂ completely eliminated naïve T_H cells (Fig. 4A), effector T_H cells became progressively less sensitive with increasing time of differentiation before addition of H₂O₂ (Fig. 4B). When viability was measured against a range of H₂O₂ concentrations, naïve T_H cells had an IC₅₀ value significantly lower than that of effector T_H cells, ~40 and ~200 μM H₂O₂, respectively (Fig. 4, C and D). A low concentration of H₂O₂ (1 μM) slightly increased the viability of effector T_H cells (Fig. 4D; *P* = 0.054). Furthermore, we measured the amount of interleukin-2 (IL-2) secreted into the external medium by T_H cells treated with 100 μM H₂O₂ 24 hours before

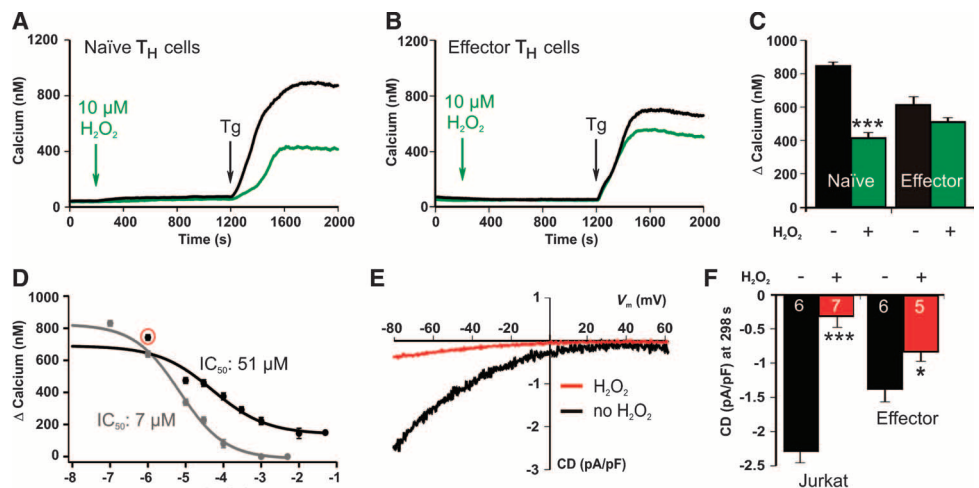


Fig. 3. Naïve and effector T_H cells show differential redox sensitivities. (A and C) [Ca²⁺]_i and Δ[Ca²⁺]_i in naïve T_H iso-cells and (B and C) in effector T_H iso-cells. Cells defined as iso-cells were selected for resting [Ca²⁺]_i between 30 and 80 nM. Green, 10 μM H₂O₂, *n* = 114 for naïve and 189 for effector; black, no H₂O₂, *n* = 442 for naïve and 154 for effector. (D) Dependence of Δ[Ca²⁺]_i on [H₂O₂] for the Tg-triggered effect in naïve (gray) and effector T_H cells (black). The red circle denotes an increased Δ[Ca²⁺]_i of effector T_H cells with 1 μM H₂O₂ compared to control. (E) I_{CRAC} current-voltage relationships from Jurkat T cells. Black trace, untreated; red trace, 500 μM H₂O₂. (F) Quantification of average I_{CRAC} CDs in Jurkat T cells and effector T_H cells. Black, untreated; red, 500 μM H₂O₂. Numbers within the bars indicate the number of cells. **P* < 0.05, ****P* < 0.001, unpaired Student's *t* test.

or in control cells. Naïve T_H cells secreted negligible levels of IL-2 (Table 1). In contrast, effector T_H cells secreted measurable amounts of IL-2, which were reduced by pretreatment with 100 μ M H_2O_2 . This inhibition progressively decreases with differentiation (Table 1).

Differential *Orai3* expression modulates redox sensitivity

Given the differential redox regulation of ORAI1 and ORAI3, we tested if the reduced redox sensitivity of effector T_H cells could be explained by a relative up-regulation of *Orai3* expression. We performed quantitative reverse transcription polymerase chain reaction (qRT-PCR) from naïve

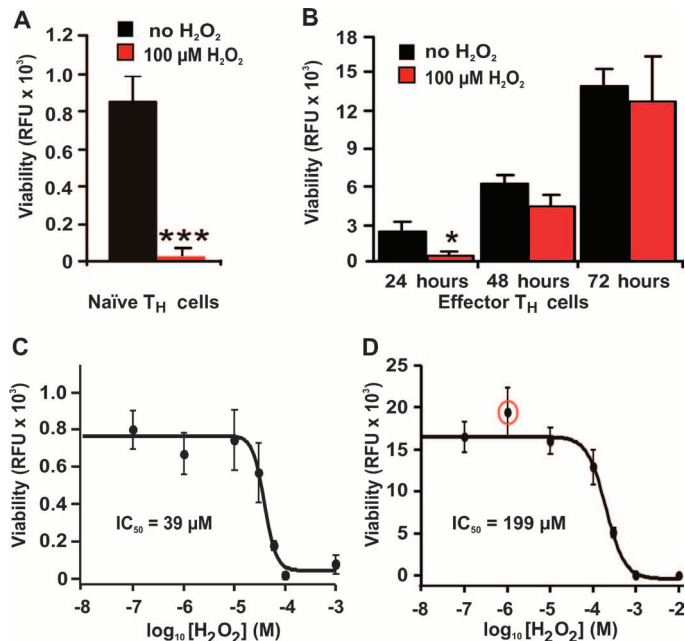


Fig. 4. H_2O_2 differentially affects the viability of T_H cells. (A) Viability of naïve T_H cells without (black) and with (red) 100 μ M H_2O_2 measured in relative fluorescence units (RFU). (B) Viability of effector T_H cells at different time points of differentiation without (black) and with (red) 100 μ M H_2O_2 . (C) H_2O_2 dose dependence of naïve T_H cell viability. (D) H_2O_2 dose dependence of effector T_H cells treated with H_2O_2 72 hours after bead stimulation. The red circle denotes an increased viability of effector T_H cells with 1 μ M H_2O_2 compared to control. Viability was determined 24 hours after the addition of H_2O_2 . * $P < 0.05$, *** $P < 0.001$, unpaired Student's t test.

Table 1. Concentration of secreted IL-2 (ng/ml). Supernatants of naïve and effector T_H cells were collected and IL-2 concentrations were determined with an IL-2–specific ELISA. Values are means \pm SEM of three (effector) or four donors (naïve). The P values were calculated with paired two-sided Student's t test. N.S., not significant.

	Naïve T_H cells	Effector T_H cells		
		24 hours	48 hours	72 hours
0 μ M H_2O_2	0.011 \pm 0.006	6.09 \pm 1.2	11.8 \pm 0.9	13.5 \pm 1.8
100 μ M H_2O_2	0.004 \pm 0.0005	1.33 \pm 0.7	6.88 \pm 2.2	10.83 \pm 1.9
% Inhibition by 100 μ M H_2O_2		78	42	20
P value	N.S.	0.013	0.059	0.45

and effector T_H cells and found that *Orai3* showed higher mRNA expression in effector than in naïve T_H cells, whereas expression of *Orai1* was not significantly changed (Fig. 5A). The relative ratio of *Orai1/Orai3* expression was thus significantly decreased after 3 days of differentiation (Fig. 5B). We then transfected HEKS1 cells with an *Orai1/Orai3* ratio of 5:1 to mimic the appearance of low amounts of *Orai3* in native systems and measured the percentage of current inhibition by H_2O_2 . Coexpression of *Orai3* significantly reduced current inhibition, indicating that changing the *Orai1/Orai3* mRNA ratio can alter H_2O_2 sensitivity (Fig. 5C). These data suggest that the presence of ORAI3 subunits either by themselves or in a heteromeric complex with ORAI1 alters H_2O_2 sensitivity.

If up-regulation of *Orai3* causes effector T_H cells to become less sensitive toward extracellular ROS, down-regulation of *Orai3* expression should render them more sensitive. To test this hypothesis, we transfected T_H cells 24 hours after bead stimulation either with a pool of two siRNAs against *Orai3* (O3 siRNA) or with a control siRNA (CTRL siRNA). *Orai3* mRNA levels were down-regulated by O3 siRNA, whereas *Orai1* mRNA levels were unaffected, as analyzed by qRT-PCR (Fig. 5D). The relative ratio of *Orai1/Orai3* expression was significantly increased in the O3 siRNA–treated cells when compared to the CTRL siRNA–treated cells (Fig. 5E). We confirmed the down-regulation of the ORAI3 protein with O3 siRNA by analyzing protein levels of overexpressed ORAI3-GFP in HEKS1 cells (fig. S4). We next measured the sensitivity of Tg-induced Ca^{2+} increase toward 100 μ M H_2O_2 . Compared to effector cells treated with CTRL siRNA, O3 siRNA–treated cells were significantly more inhibited by 100 μ M H_2O_2 (Fig. 5F), thus confirming our prediction. We conclude that up-regulation of *Orai3* expression is necessary to change the redox sensitivity of CRAC-dependent Ca^{2+} influx in T cells.

To test whether effector T_H cells develop additional protective mechanisms against oxidative stress that may explain the reduced sensitivity of the initial H_2O_2 -induced Ca^{2+} influx, we determined the concentration of two major cellular antioxidants, glutathione and catalase. The concentrations of both reduced and total glutathione were increased in effector compared to naïve T_H cells (fig. S5, A and B). Moreover, the activity of the H_2O_2 scavenger catalase was also significantly increased (fig. S4C). Both these results point toward a protection of redox-sensitive proteins containing cytosolic reactive cysteines, thereby reducing the initial effect of H_2O_2 on $[Ca^{2+}]_i$.

DISCUSSION

Our data indicate that oxidation inhibits ORAI1 but not ORAI3 channel activity. This differential sensitivity can be largely explained by the presence of the extracellular cysteine Cys¹⁹⁵ in ORAI1, which is absent in ORAI3. Although Cys¹⁹⁵ is positioned close to the membrane, our data argue that it is reactive and amenable to oxidation. Mutation of Cys¹⁹⁵ to

serine did not reduce current size or change the shape of the current-voltage relationship and thus does not lead to a major alteration of the selectivity filter (E^{106} , E^{190}) [(38, 39), see also (40)]. ORAI3 channels were not inhibited by H_2O_2 , which was not only due to small current size because

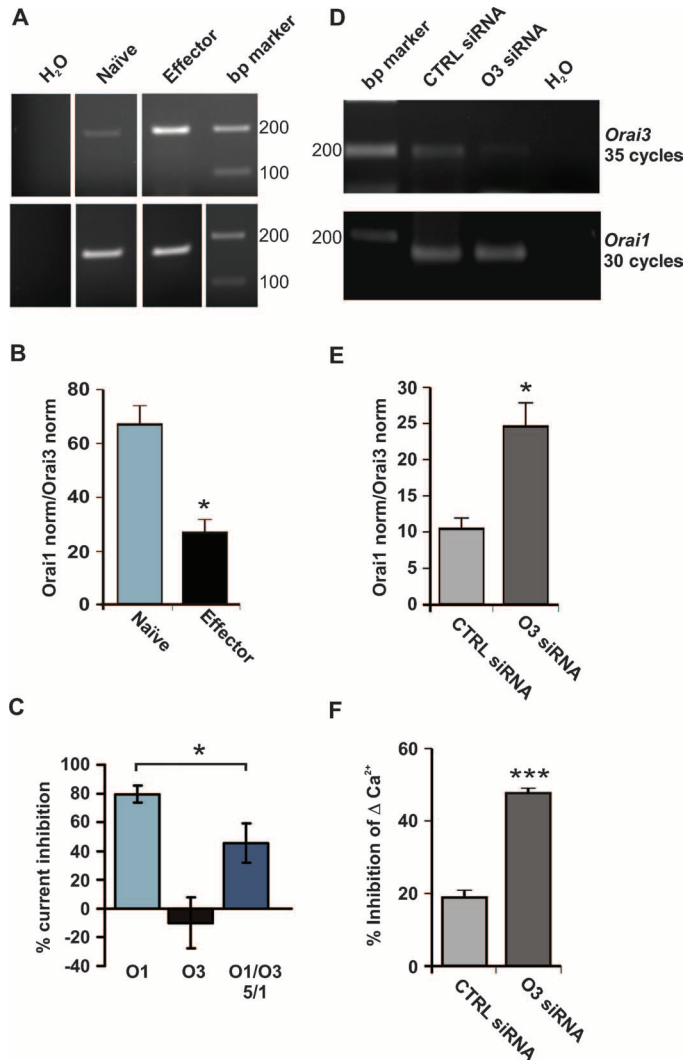


Fig. 5. ORAI3 reduces redox sensitivity of CRAC channels in effector T_H cells. (A and B) qRT-PCR analyses of *Orai1* and *Orai3* expression in naïve and 72- to 96-hour effector T_H cells. (B) Ratio of *Orai1/Orai3* expression each normalized to RNA polymerase in naïve and effector T_H cells. (C) Percent inhibition (CD 1 mM H_2O_2 /average unblocked CD) for HEK293 cells expressing *Orai1*, *Orai3*, or *Orai1* together with *Orai3* at a ratio of 5:1. The total amount of DNA transfected was 1 μ g for each condition. (D and E) qRT-PCR analyses of *Orai1* and *Orai3* expression in naïve and 72- to 96-hour effector T_H cells transfected with O3 siRNA or CTRL siRNA. (E) Ratio of *Orai1/Orai3* expression each normalized to RNA polymerase in CTRL siRNA- or O3 siRNA-transfected effector T_H cells. (F) Percent inhibition ($\Delta[Ca^{2+}]_i$ 100 μ M H_2O_2 /average untreated $\Delta[Ca^{2+}]_i$) for effector T_H cells transfected with CTRL siRNA or O3 siRNA. For CTRL: $n = 548$ ($-H_2O_2$), 675 ($+H_2O_2$); for O3: $n = 556$ ($-H_2O_2$), 486 ($+H_2O_2$). * $P < 0.05$, *** $P < 0.001$, unpaired Student's t test. DNA ladder bands shown (A and D) are 200 and 100 bp.

introduction of a cysteine in the homologous position (G170C) retained small currents that were now inhibited by H_2O_2 . Current inhibition required preincubation with H_2O_2 and thus is not likely to act as an open pore blocker (fig. S1). Instead, oxidation of cysteines may lock the pore in the closed configuration, reduce single-channel conductance, the ability of ORAI1 to be effectively activated by STIM1, or the formation and/or number of active ORAI1 channels.

We also found that primary T_H cells from human blood donors were affected by changes in the redox state of the environment in multiple ways and that differentiation of naïve into effector T_H cells changed the threshold of these modifications. Addition of H_2O_2 led to an immediate increase in $[Ca^{2+}]_i$ (initial effect) that was mediated through the activation of nonselective cation channels, possibly TRPM. T_H cell differentiation shifted the activating EC_{50} values from ~ 130 to ~ 740 μ M. Because TRPM2 channels are activated by cytosolic second messengers such as cyclic adenosine diphosphate (ADP) ribose (41, 42) whose turnover rates are regulated by the oxidative stress-activated poly(ADP-ribose) polymerase (PARP-1) (43), up-regulation of cytosolic antioxidants (fig. S4) may provide a negative feedback mechanism for this pathway.

We cannot exclude a partial inhibition of Tg-induced increase in $[Ca^{2+}]_i$ due to preceding membrane depolarization. However, the patch-clamp analyses of heterologously expressed ORAI1, Jurkat T cells, and effector T cells demonstrated an inhibitory effect on the channels themselves. There was also an up-regulation of *Orai3* in effector T_H cells, and coexpression of *Orai1* and *Orai3* reduced redox sensitivity when expressed in HEK293 cells (Fig. 5). Knockdown of *Orai3* in human effector T_H cells rendered Ca^{2+} influx again more redox sensitive and provides further support for direct redox regulation of the channels.

ORAI3 may work alone or in a heteromeric complex with ORAI1. Heteromeric ORAI1-ORAI3 channel assembly with a distinct selectivity profile has recently been described as a means not only to tune Ca^{2+} selectivity of store-operated Ca^{2+} entry (18), but also to generate channels activated independently of store depletion by arachidonic acid (44).

The up-regulation of *Orai3* and other cytosolic antioxidants suggests that effector T_H cells have developed adaptive mechanisms to both tune Ca^{2+} influx and scavenge increased intracellular ROS to respond to oxidative stress. Increased concentrations of ROS within injured or inflamed tissues can create gradients of ROS that, at low concentrations (nanomolar to low micromolar), enhance proliferation and cytokine production of effector T_H cells (45–47) and thus may act as chemotactic signals (26). This enhancement could be due to an increase in $[Ca^{2+}]_i$ (compare $[Ca^{2+}]_i$ and viability at 1 μ M H_2O_2 against control for effector T_H cells; red circles in Figs. 3D and 4D). In regions of H_2O_2 concentrations between ~ 10 and ~ 300 μ M, T cells will already undergo partial CRAC channel inhibition that will not yet affect their viability and cytokine production (32, 48), but may offset increases in $[Ca^{2+}]_i$ due to activation of TRPM channels. By up-regulation of ORAI3, effector T_H cells would be able to tune their Ca^{2+} influx to continue proliferation and cytokine production in more oxidizing conditions. The *Orai3* gene is the most recent addition to the *Orai* family and is present only in mammals (49), suggesting that ORAI3-dependent redox tuning might not take place in lower vertebrates. Local ROS concentrations might reach even higher levels through increased phagocytic activity, mitochondrial dysfunction, and massive activation of T cell receptor (TCR)-mediated signaling (19, 30). This could then ultimately activate TRPM channels (36, 37, 42), release Ca^{2+} from intracellular stores (50), increase protein phosphorylation levels (30), and eventually lead to apoptosis and tissue damage (36, 51, 52).

Further investigations are necessary to elucidate the complex balance between physiological and pathological effects of oxidation and to test the role of dysregulation of *Orai* channel expression in disease.

MATERIALS AND METHODS

Chemicals

All chemicals were purchased from Sigma unless indicated otherwise.

Cell culture and isolation of primary CD4⁺ T_H cells

E6-1 Jurkat T cell line (American Type Culture Collection) and THP-1 monocyte cell line were grown in RPMI. HEKS1 cells were grown in Dulbecco's modified Eagle's medium (DMEM) supplemented with 10% fetal calf serum and penicillin-streptomycin at 37°C and 5% CO₂. Human T_H cells were isolated from leukocyte reduction filters and collected by back-flushing the filter with 60 ml of Hanks' balanced salt solution (HBSS; PAA, 15-009). Peripheral blood lymphocytes (PBLs) were isolated by a density gradient centrifugation at 450g for 30 min at room temperature (Ficoll-Paque PLUS, Amersham Biosciences, 17144002) in 50-ml Leucosep tubes (Greiner, 227290). The PBL layer was washed in HBSS. Remaining red blood cells were removed by the addition of 1 ml of lysis buffer [155 mM NH₄Cl, 10 mM KHCO₃, 0.1 mM EDTA (pH 7.3)] for 1 min. After lysis, cells were washed with HBSS [200g, 10 min at room temperature (RT)]. For further purification, PBLs were resuspended in phosphate-buffered saline (PBS) and 0.5% bovine serum albumin, and CD4⁺ T cells were negatively isolated with the CD4⁺ Negative Isolation Kit (to avoid prestimulation) from Invitrogen (113.17D), following the manufacturer's instruction (32).

Constructs and transfection

hOrai1 and *hOrai3* constructs were subcloned into pCAGGS-IRES-GFP. Mutagenesis was performed by means of Quickchange (Stratagene) with an *Orai1*-SmaI fragment in pBluescript as a template. The mutated SmaI fragment was excised and cloned into mEGFP-Orai1 pMAX vector (Lonza) with a deleted SmaI vector site. This construct served as a template to reclone the full-length mutants into pCAGGS-IRES-GFP. For creating triple mutants, mutant SmaI fragments were used as a template. All constructs were confirmed by sequencing. For transfection, 1 µg of DNA was electroporated into HEKS1 cells with the Nucleofector II electroporator (Lonza) and Nucleofector kit (Lonza). Cells were transfected according to the manufacturer's instructions and seeded 24 hours before measurements.

Small interfering RNA transfection

Orai3 small interfering RNAs (siRNAs) Hs_TMEM142C_2 [sense: 5' r(OMeC-OMeA-CCAGUGGCUACCUCC)d(CUU)d(OMeA-OMeT-OMeT) 3'; antisense: 3' r(OMeG-OMeT-GGUCACCGAUGGAGGGAA)d(U) 5' (#SI04174191)] and Hs_TMEM142C_5 [sense: 5' r(OMeT-OMeC-CUUAGCCCUUGAAAU)d(ACA)d(OMeA-OMeT-OMeT) 3'; antisense: 3' r(OMeA-OMeG-GAAUCGGGAACUUUAUGU)d(U) 5' (#SI04348876)] and CTRL siRNA (#1022076) from Qiagen were chemically modified by the addition of two deoxy or methoxy groups (to increase stability) (53). CD4⁺ T_H cells were stimulated with self-made beads coated with antibodies against CD3 and CD28 (32). Cells (5 × 10⁶) were nucleofected with 8.0 µl of siRNA or CTRL siRNA (20 µM) using Nucleofector technology (Lonza) according to the manufacturer's instructions. For down-regulation of *Orai3*, a 1:1 mixture of both *Orai3* siRNAs was used.

Fluorescence-based Ca²⁺ imaging

External solution (buffer A) contained 155 mM NaCl, 4.5 mM KCl, 2 mM MgCl₂, 10 mM D-glucose, 5 mM Hepes (pH 7.4 with NaOH), and CaCl₂ at 0.5 mM (for HEKS1 cells) or 1 mM (for T cells). Cells were loaded with 1 µM Fura 2-AM. Images were analyzed with TILLVision software.

[Ca²⁺]_i was estimated from the relation $[Ca^{2+}]_i = K^*(R - R_{min})/(R_{max} - R)$, where the values of K^* , R_{min} , and R_{max} were determined from an in situ calibration of Fura 2 in T_H and HEK293 cells as described in (54, 55). To exclude nonspecific effects of H₂O₂ on Ca²⁺ measurements, we analyzed the redox properties of Fura 2 (56).

Electrophysiology: T cells

Patch-clamp experiments were performed in the whole-cell configuration with fire-polished patch pipettes (3 to 5 megohm). Pipette and cell capacitance were electronically compensated before each voltage ramp with an EPC-9 patch-clamp amplifier controlled by Pulse 8.4 or Patchmaster software (HEKA). Membrane currents were sampled at 3 kHz and filtered at 1 kHz. Whole-cell currents were elicited by 200-ms voltage ramps from -100 to +100 mV from a holding potential of 0 mV. To measure leak currents, 20 voltage ramps were applied within the first 5 s after establishment of the whole-cell configuration, followed by ramps applied every second. All voltages were corrected for a liquid junction potential of -12 mV. For leak current correction, the ramp current before CRAC activation was subtracted. The solutions used for measurements of I_{CRAC} were as follows: pipette: 140 mM cesium aspartate, 10 mM NaCl, 5 mM MgCl₂, 10 mM EGTA, and 10 mM Hepes (pH 7.2 with CsOH); bath solution: 155 mM NaCl, 4.5 mM KCl, 10 mM CaCl₂, 2 mM MgCl₂, 10 mM D-glucose, and 5 mM Hepes (pH 7.4 with NaOH). H₂O₂-induced currents were measured as in (37).

HEK cells

Whole-cell currents were elicited by 50-ms ramps from -150 to +150 mV at 0.5 Hz from a holding potential of 0 mV. For leak current correction, the ramp current before ORAI activation was subtracted. Cells with an initial inward current greater than -10 pA/pF (-130 mV) and significant outliers ($P < 0.01$, Grubb's test) were excluded. Voltages were corrected for a liquid junction potential of -10 mV. The internal solution contained 120 mM cesium glutamate, 20 mM cesium-BAPTA [1,2-bis(2-aminophenoxy)ethane-*N,N,N',N'*-tetraacetic acid], 3 mM MgCl₂, 0.05 mM IP₃, and 10 mM Hepes (pH 7.2 with CsOH). The external solution contained 120 mM NaCl, 10 mM CaCl₂, 2 mM MgCl₂, 10 mM TEA-HCl (tetraethylammonium chloride), 10 mM glucose, and 10 mM Hepes (pH 7.2 with NaOH). Inward and outward currents were analyzed at -80 and +80 mV ramp potential for both T cells and HEK cells.

DTNB-2Bio labeling assay

The DTNB-2Bio labeling assay was performed as previously described with modifications (57). HEK cells transfected with EGFP-hOrai1, EGFP-hOrai1_C195S, EGFP-hOrai1_C126S/C143S/C195S, or EGFP-Orai3 (~7 × 10⁶) were washed with PBS. Membranes were permeabilized with 0.001% digitonin for 5 min. Cells were collected and incubated in Hepes-buffered saline (HBS) solution with or without 1 mM H₂O₂ for 15 min followed by 50 µM DTNB-2Bio for 40 min at RT. Cells were washed with HBS and lysed in radioimmunoprecipitation assay (RIPA) buffer (pH 8.0) containing 150 mM NaCl, 1% Nonidet P-40, 0.5% sodium deoxycholate, 0.1% SDS, 50 mM Tris, 1 mM phenylmethylsulfonyl fluoride, aprotinin (5 µg/ml) and leupeptin (1 µg/ml). Cell lysates were incubated with NeutrAvidin-Plus beads (Thermo-Scientific) overnight at 4°C with constant shaking. Beads were rinsed five times with RIPA buffer by centrifugation at 15,000 rpm for 1 min. Proteins were eluted in RIPA buffer containing 50 mM dithiothreitol (DTT) for 60 min and denatured in SDS sample buffer containing 50 mM DTT for 30 min at room temperature. Proteins were analyzed by 7.5% SDS-polyacrylamide gel electrophoresis (SDS-PAGE), transferred to membrane, and detected with an antibody against GFP (Clontech).

Cell viability and proliferation

Measurements were carried out in 96-well cell culture plates (BD). Each data point was measured in triplicate. Naïve T_H cells (50,000) were seeded in a total volume of 200 µl of AIM V medium. For effector T_H cell measurements, these were then activated with antibody (against CD3 and CD28)-coated beads (Invitrogen) and incubated at 37°C, 5% CO₂, and 95% humidity. Living cells were detected with the CellTiter-Blue assay (Promega) (32).

Measurements of IL-2 secretion

After proliferation was measured, 96-well plates were centrifuged (150g, 7 min, RT) and supernatants were collected and frozen for later use. Different dilutions of the supernatants and of an IL-2 standard were then analyzed in duplicates with an ELISA assay (DuoSet; DY202, R&D Systems) according to the manufacturer's instructions. Supernatants from four (naïve) and three (effector) T_H cell donors were analyzed.

qRT-PCR

Total RNA was isolated from naïve and effector T_H cells [(2.5 to 8.0) × 10⁶ each, stimulated with antibody (against CD3 and CD28)-coated beads for 72 hours] from five donors. Isolated total RNA (1.5 µl) or total RNA (1 µg) was used for reverse transcription. Complementary DNA (cDNA; 0.5 µl) and 300 nM primer were used in a QuantiTect SYBR green kit (Qiagen). PCR conditions were as follows: 15 min at 94°C; 45 cycles, 30 s at 94°C; 45 s at 58°C; and 30 s at 72°C with a final cycle (60 s at 95°C, 30 s at 55°C, and 30 s at 95°C) using the MX3000 cyclor (Stratagene). Primers were designed as described in <http://frodo.wi.mit.edu/>. Expression of *Orai1* and *Orai3* was normalized to the expression of the housekeeping gene RNA polymerase II (NM_000937). Relative expression was calculated according to the ΔCT method (2^{-ΔCT}). CT values were determined by the MX3000 software. The reliability of the housekeeping gene was also confirmed by a second house keeping gene, TATA box binding protein (NM_003194). To calculate primer efficiencies, raw fluorescence data from MX3000 measurements were analyzed by fitting the early exponential phase of the reaction and correcting the CT value accordingly (IgorPro macro). Primer sequences for *Orai1* were 5' atgagcctcaacgagcact3' and 5'gtggtagtcgtggtcag3' [159 base pairs (bp)] and for *Orai3* were 5'gtaccggggatctgtgca3' and 5'ggtactctgtgctactct3' (193 bp). All primer pairs span an intron-exon boundary to avoid amplification of genomic DNA. Amplification products were confirmed by DNA sequencing (MWG).

Determination of glutathione and catalase activity

One million naïve or effector T_H cells (per sample) were lysed by consecutive freezing and thawing, centrifuged for 10 min at 14,000 rpm, resuspended in PBS buffer, and kept on ice. Total glutathione was determined with the fluorescent dye monochlorobimane (MCB, 100 µM). The reaction was catalyzed by glutathione S-transferase (GST; 1 U/ml). All measurements were performed with a microplate reader (GeniosPro, Tecan). Reduced glutathione was measured with the fluorescent dye o-phthalaldehyde (OPA, 5 mg/ml). Cell lysates were deproteinized with 6 M perchloric acid for 5 min and centrifuged for 5 min at 14,000 rpm. pH was restored (7–11) with 3 M NaOH. Supernatants were used for further measurements. Catalase activity was determined with a spectrophotometer (Ultrospec 2100) using absorption of H₂O₂ at 240 nm according to Beers and Sizer (58). One million cells were lysed in 120 µl of PBS buffer containing 0.1% Triton X-100. Lysates were centrifuged for 10 min at 14,000 rpm and supernatants were measured with quartz cuvettes (IQS). The supernatant (100 µl) was mixed with 2.9 ml of PBS buffer containing 10 mM H₂O₂. Absorbance at 240 nm (A₂₄₀) was

recorded every 30 s for 10 min. The final catalase concentration per cell was calculated according to a standard curve determined with different concentrations (units per milliliter) of recombinant catalase as reference.

Data analysis and statistics

Data were analyzed with TILL Vision (TILL Photonics), Fitmaster 2.35 (HEKA), Igor Pro (Wavemetrics), and Microsoft Excel (Microsoft). Data are means ± SEM unless otherwise indicated. Asterisks indicate significance: **P* < 0.05, ***P* < 0.01, ****P* < 0.001 (unpaired, two-sided Student's *t* test). Primary human T_H cells were isolated from at least two different healthy donors. For each condition, at least three experiments were performed. For calculation of IC₅₀ values, data were fitted with Hill's equations (least-squares method).

SUPPLEMENTARY MATERIALS

www.sciencesignaling.org/cgi/content/full/3/115/ra24/DC1

Fig. S1. Activated CRAC channels are not inhibited by H₂O₂.

Fig. S2. H₂O₂ effect on Orai2 and current/voltage relationships of Orai1WT, Orai1TM, Orai1C195S and Orai3WT.

Fig. S3. H₂O₂ activates nonselective ion channels.

Fig. S4. *Orai3* siRNA down-regulates Orai3 protein.

Fig. S5. Relative amounts and activity of cellular antioxidants in naïve and effector T_H cells.

REFERENCES AND NOTES

1. M. J. Berridge, P. Lipp, M. D. Bootman, The versatility and universality of calcium signalling. *Nat. Rev. Mol. Cell Biol.* **1**, 11–21 (2000).
2. J. W. Putney Jr., A model for receptor-regulated calcium entry. *Cell Calcium* **7**, 1–12 (1986).
3. M. Hoth, R. Penner, Depletion of intracellular calcium stores activates a calcium current in mast cells. *Nature* **355**, 353–356 (1992).
4. A. B. Parekh, J. W. Putney Jr., Store-operated calcium channels. *Physiol. Rev.* **85**, 757–810 (2005).
5. S. L. Zhang, Y. Yu, J. Roos, J. A. Kozak, T. J. Deerinck, M. H. Ellisman, K. A. Stauderman, M. D. Cahalan, STIM1 is a Ca²⁺ sensor that activates CRAC channels and migrates from the Ca²⁺ store to the plasma membrane. *Nature* **437**, 902–905 (2005).
6. J. Liou, M. L. Kim, W. D. Heo, J. T. Jones, J. W. Myers, J. E. Ferrell Jr., T. Meyer, STIM is a Ca²⁺ sensor essential for Ca²⁺-store-depletion-triggered Ca²⁺ influx. *Curr. Biol.* **15**, 1235–1241 (2005).
7. S. Feske, Y. Gwack, M. Prakriya, S. Srikanth, S. H. Puppel, B. Tanasa, P. G. Hogan, R. S. Lewis, M. Daly, A. Rao, A mutation in Orai1 causes immune deficiency by abrogating CRAC channel function. *Nature* **441**, 179–185 (2006).
8. M. Vig, C. Peinelt, A. Beck, D. L. Koomoa, D. Rabah, M. Koblan-Huberson, S. Kraft, H. Turner, A. Fleig, R. Penner, J. P. Kinet, CRACM1 is a plasma membrane protein essential for store-operated Ca²⁺ entry. *Science* **312**, 1220–1223 (2006).
9. S. L. Zhang, A. V. Yeromin, X. H. Zhang, Y. Yu, O. Safrina, A. Penna, J. Roos, K. A. Stauderman, M. D. Cahalan, Genome-wide RNAi screen of Ca²⁺ influx identifies genes that regulate Ca²⁺ release-activated Ca²⁺ channel activity. *Proc. Natl. Acad. Sci. U.S.A.* **103**, 9357–9362 (2006).
10. C. Y. Park, P. J. Hoover, F. M. Mullins, P. Bachhawat, E. D. Covington, S. Raunser, T. Walz, K. C. Garcia, R. E. Dolmetsch, R. S. Lewis, STIM1 clusters and activates CRAC channels via direct binding of a cytosolic domain to Orai1. *Cell* **136**, 876–890 (2009).
11. M. Muik, M. Fahrner, I. Derler, R. Schindl, J. Bergsmann, I. Frischauf, K. Groschner, C. Romanin, A cytosolic homomerization and a modulatory domain within STIM1 C terminus determine coupling to Orai1 channels. *J. Biol. Chem.* **284**, 8421–8426 (2009).
12. S. Feske, Calcium signalling in lymphocyte activation and disease. *Nat. Rev. Immunol.* **7**, 690–702 (2007).
13. R. S. Lewis, The molecular choreography of a store-operated calcium channel. *Nature* **446**, 284–287 (2007).
14. S. A. Gross, U. Wissenbach, S. E. Philipp, M. Freichel, A. Cavalie, V. Flockerzi, Murine Orai2 splice variants form functional Ca²⁺ release-activated Ca²⁺ (CRAC) channels. *J. Biol. Chem.* **282**, 19375–19384 (2007).
15. Y. Gwack, S. Srikanth, S. Feske, F. Cruz-Guilloty, M. Oh-hora, D. S. Neems, P. G. Hogan, A. Rao, Biochemical and functional characterization of Orai proteins. *J. Biol. Chem.* **282**, 16232–16243 (2007).
16. I. Frischauf, R. Schindl, I. Derler, J. Bergsmann, M. Fahrner, C. Romanin, The STIM/Orai coupling machinery. *Channels (Austin)* **2**, 261–268 (2008).

17. A. Lis, C. Peinelt, A. Beck, S. Parvez, M. Monteilh-Zoller, A. Fleig, R. Penner, CRACM1, CRACM2, and CRACM3 are store-operated Ca^{2+} channels with distinct functional properties. *Curr. Biol.* **17**, 794–800 (2007).
18. R. Schindl, I. Frischauf, I. Bergsmann, M. Muik, I. Derler, B. Lackner, K. Groschner, C. Romanin, Plasticity in Ca^{2+} selectivity of Orai1/Orai3 heteromeric channel. *Proc. Natl. Acad. Sci. U.S.A.* **106**, 19623–19628 (2009).
19. W. Dröge, Free radicals in the physiological control of cell function. *Physiol. Rev.* **82**, 47–95 (2002).
20. S. G. Rhee, Cell signaling: H_2O_2 , a necessary evil for cell signaling. *Science* **312**, 1882–1883 (2006).
21. J. D. Lambeth, NOX enzymes and the biology of reactive oxygen. *Nat. Rev. Immunol.* **4**, 181–189 (2004).
22. A. A. Starkov, The role of mitochondria in reactive oxygen species metabolism and signaling. *Ann. N.Y. Acad. Sci.* **1147**, 37–52 (2008).
23. I. Fridovich, Fundamental aspects of reactive oxygen species, or what's the matter with oxygen? *Ann. N.Y. Acad. Sci.* **893**, 13–18 (1999).
24. C. F. Nathan, R. K. Root, Hydrogen peroxide release from mouse peritoneal macrophages: Dependence on sequential activation and triggering. *J. Exp. Med.* **146**, 1648–1662 (1977).
25. S. Mueller, Sensitive and nonenzymatic measurement of hydrogen peroxide in biological systems. *Free Radic. Biol. Med.* **29**, 410–415 (2000).
26. P. Niethammer, C. Grabher, A. T. Look, T. J. Mitchison, A tissue-scale gradient of hydrogen peroxide mediates rapid wound detection in zebrafish. *Nature* **459**, 996–999 (2009).
27. X. Liu, J. L. Zweier, A real-time electrochemical technique for measurement of cellular hydrogen peroxide generation and consumption: Evaluation in human polymorphonuclear leukocytes. *Free Radic. Biol. Med.* **31**, 894–901 (2001).
28. S. M. Davidson, M. R. Duchon, Calcium microdomains and oxidative stress. *Cell Calcium* **40**, 561–574 (2006).
29. C. Amatore, S. Arbault, C. Bouton, K. Coffi, J. C. Drapier, H. Ghandour, Y. Tong, Monitoring in real time with a microelectrode the release of reactive oxygen and nitrogen species by a single macrophage stimulated by its membrane mechanical depolarization. *ChemBiochem* **7**, 653–661 (2006).
30. M. Reth, Hydrogen peroxide as second messenger in lymphocyte activation. *Nat. Immunol.* **3**, 1129–1134 (2002).
31. J. Soboloff, M. A. Spassova, X. D. Tang, T. Hewavitharana, W. Xu, D. L. Gill, Orai1 and STIM reconstitute store-operated calcium channel function. *J. Biol. Chem.* **281**, 20661–20665 (2006).
32. E. C. Schwarz, C. Kummerow, A. S. Wenning, K. Wagner, A. Sappok, K. Waggerhauser, D. Griesemer, B. Strauss, M. J. Wolfs, A. Quintana, M. Hoth, Calcium dependence of T cell proliferation following focal stimulation. *Eur. J. Immunol.* **37**, 2723–2733 (2007).
33. K. Hill, C. D. Benham, S. McNulty, A. D. Randall, Flufenamic acid is a pH-dependent antagonist of TRPM2 channels. *Neuropharmacology* **47**, 450–460 (2004).
34. M. D. Cahalan, K. G. Chandy, The functional network of ion channels in T lymphocytes. *Immunol. Rev.* **231**, 59–87 (2009).
35. Y. Sano, K. Inamura, A. Miyake, S. Mochizuki, H. Yokoi, H. Matsushime, K. Furuichi, Immuncyte Ca^{2+} influx system mediated by LTRPC2. *Science* **293**, 1327–1330 (2001).
36. M. Aarts, K. Iihara, W. L. Wei, Z. G. Xiong, M. Arundine, W. Cerwinski, J. F. MacDonald, M. Tymianski, A key role for TRPM7 channels in anoxic neuronal death. *Cell* **115**, 863–877 (2003).
37. Y. Hara, M. Wakamori, M. Ishii, E. Maeno, M. Nishida, T. Yoshida, H. Yamada, S. Shimizu, E. Mori, J. Kudoh, N. Shimizu, H. Kurose, Y. Okada, K. Imoto, Y. Mori, LTRPC2 Ca^{2+} -permeable channel activated by changes in redox status confers susceptibility to cell death. *Mol. Cell* **9**, 163–173 (2002).
38. A. V. Yeromin, S. L. Zhang, W. Jiang, Y. Yu, O. Safrina, M. D. Cahalan, Molecular identification of the CRAC channel by altered ion selectivity in a mutant of Orai. *Nature* **443**, 226–229 (2006).
39. M. Vig, A. Beck, J. M. Billingsley, A. Lis, S. Parvez, C. Peinelt, D. L. Koomoa, J. Soboloff, D. L. Gill, A. Fleig, J. P. Kinet, R. Penner, CRACM1 multimers form the ion-selective pore of the CRAC channel. *Curr. Biol.* **16**, 2073–2079 (2006).
40. B. A. McNally, M. Yamashita, A. Engh, M. Prakriya, Structural determinants of ion permeation in CRAC channels. *Proc. Natl. Acad. Sci. U.S.A.* **106**, 22516–22521 (2009).
41. M. Kolisek, A. Beck, A. Fleig, R. Penner, Cyclic ADP-ribose and hydrogen peroxide synergize with ADP-ribose in the activation of TRPM2 channels. *Mol. Cell* **18**, 61–69 (2005).
42. B. A. Miller, The role of TRP channels in oxidative stress-induced cell death. *J. Membr. Biol.* **209**, 31–41 (2006).
43. B. Buelow, Y. Song, A. M. Scharenberg, The Poly(ADP-ribose) polymerase PARP-1 is required for oxidative stress-induced TRPM2 activation in lymphocytes. *J. Biol. Chem.* **283**, 24571–24583 (2008).
44. O. Mignen, J. L. Thompson, T. J. Shuttleworth, The molecular architecture of the arachidonate-regulated Ca^{2+} -selective ARC channel is a pentameric assembly of Orai1 and Orai3 subunits. *J. Physiol.* **587**, 4181–4197 (2009).
45. S. Roth, W. Dröge, Regulation of T-cell activation and T-cell growth factor (TCGF) production by hydrogen peroxide. *Cell. Immunol.* **108**, 417–424 (1987).
46. S. Tatla, V. Woodhead, J. C. Foreman, B. M. Chain, The role of reactive oxygen species in triggering proliferation and IL-2 secretion in T cells. *Free Radic. Biol. Med.* **26**, 14–24 (1999).
47. S. P. Hehner, R. Breitkreutz, G. Shubinsky, H. Unsoeld, K. Schulze-Osthoff, M. L. Schmitz, W. Dröge, Enhancement of T cell receptor signaling by a mild oxidative shift in the intracellular thiol pool. *J. Immunol.* **165**, 4319–4328 (2000).
48. C. Zitt, B. Strauss, E. C. Schwarz, N. Spaeth, G. Rast, A. Hatzelmann, M. Hoth, Potent inhibition of Ca^{2+} release-activated Ca^{2+} channels and T-lymphocyte activation by the pyrazole derivative BTP2. *J. Biol. Chem.* **279**, 12427–12437 (2004).
49. X. Cai, Molecular evolution and structural analysis of the Ca^{2+} release-activated Ca^{2+} channel subunit, Orai. *J. Mol. Biol.* **368**, 1284–1291 (2007).
50. C. Hidalgo, P. Donoso, Crosstalk between calcium and redox signaling: From molecular mechanisms to health implications. *Antioxid. Redox. Signal.* **10**, 1275–1312 (2008).
51. P. Tripathi, D. Hildeman, Sensitization of T cells to apoptosis—A role for ROS? *Apoptosis* **9**, 515–523 (2004).
52. Y. Imai, K. Kuba, G. G. Neely, R. Yaghubian-Malhami, T. Perkmann, G. van Loo, M. Ermolaeva, R. Veldhuizen, Y. H. C. Leung, H. Wang, H. Liu, Y. Sun, M. Pasparakis, M. Kopf, C. Mech, S. Bavari, J. S. M. Peiris, A. S. Slutsky, S. Akira, M. Hultqvist, R. Holmdahl, J. Nicholls, C. Jiang, C. J. Binder, J. M. Penninger, Identification of oxidative stress and Toll-like receptor 4 signaling as a key pathway of acute lung injury. *Cell* **133**, 235–249 (2008).
53. A. Mantei, S. Rutz, M. Janke, D. Kirchhoff, U. Jung, V. Patzel, U. Vogel, T. Rudel, I. Andreou, M. Weber, A. Scheffold, siRNA stabilization prolongs gene knockdown in primary T lymphocytes. *Eur. J. Immunol.* **38**, 2616–2625 (2008).
54. A. Quintana, E. C. Schwarz, C. Schwindling, P. Lipp, L. Kaestner, M. Hoth, Sustained activity of calcium release-activated calcium channels requires translocation of mitochondria to the plasma membrane. *J. Biol. Chem.* **281**, 40302–40309 (2006).
55. G. Grynkiewicz, M. Poenie, R. Y. Tsien, A new generation of Ca^{2+} indicators with greatly improved fluorescence properties. *J. Biol. Chem.* **260**, 3440–3450 (1985).
56. R. Gulaboski, C. M. Pereira, M. N. Cordeiro, A. F. Silva, M. Hoth, I. Bogeski, Redox properties of the calcium chelator Fura-2 in mimetic biomembranes. *Cell Calcium* **43**, 615–621 (2008).
57. T. Yoshida, R. Inoue, T. Morii, N. Takahashi, S. Yamamoto, Y. Hara, M. Tomimaga, S. Shimizu, Y. Sato, Y. Mori, Nitric oxide activates TRP channels by cysteine S-nitrosylation. *Nat. Chem. Biol.* **2**, 596–607 (2006).
58. R. F. Beers Jr., I. W. Sizer, A spectrophotometric method for measuring the breakdown of hydrogen peroxide by catalase. *J. Biol. Chem.* **195**, 133–140 (1952).
59. **Acknowledgments:** Research carried out for this study with human material has been approved by the local ethics committee. We are grateful to S. Kiyonaka for providing the DTNB2-Biotin and J. Soboloff for providing HEK293 cells. We thank B. Strauß, A. Ludes, and A. Armbrüster for technical assistance. **Funding:** This project was funded by the Deutsche Forschungsgemeinschaft (DFG; SFB 530, project A3, and the Graduate Programs GK1326 and GK845, to M.H. and B.A.N.) and competitive research grants from the Saarland University (HOMFOR to M.H., I.B., C.P., and B.A.N.). C.P. acknowledges funding by the DFG (PE 1478/5-1). **Author contributions:** I.B. performed all imaging experiments. D.A., C.K., B.A.N., C.P., and I.B. performed patch-clamp experiments. D.A. and B.A.N. cloned all constructs. E.C.S. contributed qRT-PCR data. D.K., N.T., and Y.M. contributed DTNB2-Bio data. I.B. and R.K. performed glutathione and catalase measurements. M.B., I.B., and D.A. conducted proliferation and IL-2 measurements. D.G. and C.P. provided initial technical support and reagents. I.B., Y.M., M.H., and B.A.N. designed experiments, analyzed the data, and wrote the paper. **Competing interests:** The authors have no conflicting financial interests.

Submitted 2 October 2009

Accepted 3 March 2010

Final Publication 30 March 2010

10.1126/scisignal.2000672

Citation: I. Bogeski, C. Kummerow, D. Al-Ansary, E. C. Schwarz, R. Koehler, D. Kozai, N. Takahashi, C. Peinelt, D. Griesemer, M. Bozem, Y. Mori, M. Hoth, B. A. Niemeyer, Differential redox regulation of ORAI ion channels: A mechanism to tune cellular calcium signaling. *Sci. Signal.* **3**, ra24 (2010).

Supplementary Materials for
**Differential Redox Regulation of ORAI Ion Channels: A Mechanism to
Tune Cellular Calcium Signaling**

Ivan Bogeski,* Carsten Kummerow, Dalia Al-Ansary, Eva C. Schwarz, Richard Koehler,
Daisuke Kozai, Nobuaki Takahashi, Christine Peinelt, Desiree Griesemer, Monika
Bozem, Yasuo Mori, Markus Hoth, Barbara A. Niemeyer*

*To whom correspondence should be addressed. E-mail: ivan.bogeski@uks.eu (I.B.);
barbara.niemeyer@uks.eu (B.A.N.)

Published 30 March 2010, *Sci. Signal.* **3**, ra24 (2010)
DOI: 10.1126/scisignal.2000672

The PDF file includes:

Fig. S1. Activated CRAC channels are not inhibited by H₂O₂.

Fig. S2. H₂O₂ effect on ORAI2 and current/voltage relationships of ORAI1WT,
ORAI1TM, ORAI1C195S and ORAI3WT.

Fig. S3. H₂O₂ activates nonselective ion channels.

Fig. S4. *Orai3* siRNA down-regulates ORAI3 protein.

Fig. S5. Relative amounts and activity of cellular antioxidants in naïve and effector
T_H cells.

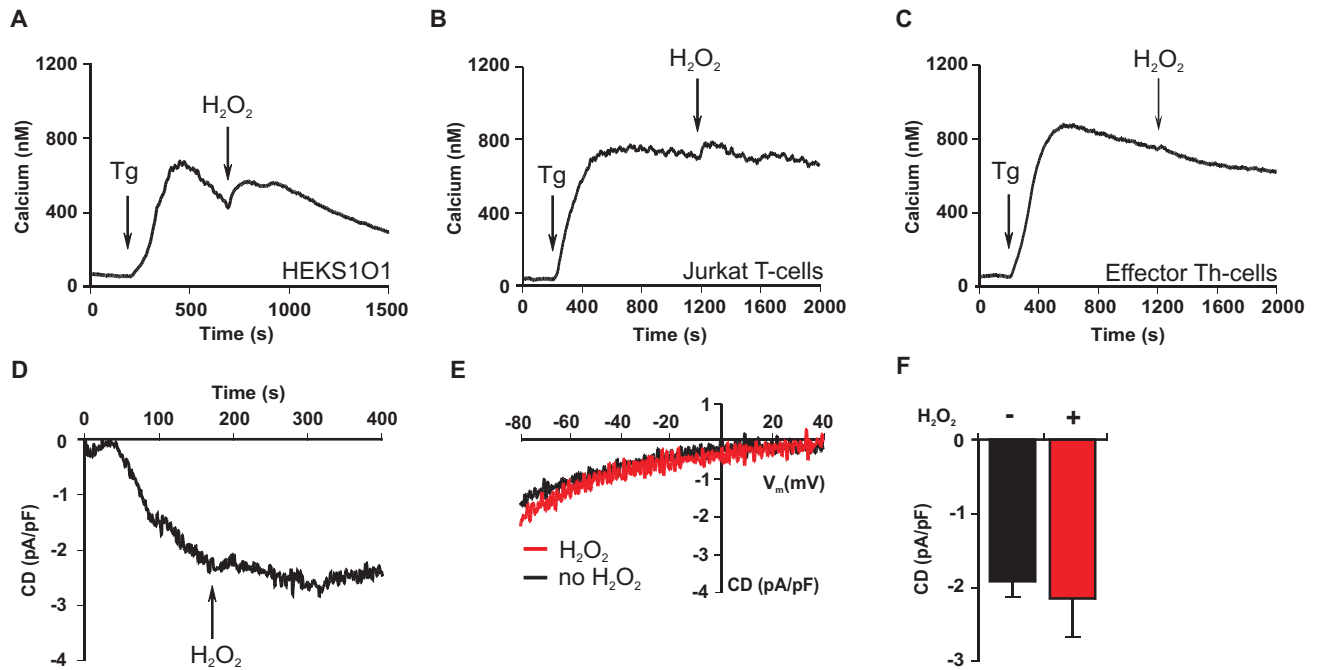


Figure S1: Activated CRAC channels are not inhibited by H₂O₂

[Ca²⁺]_i measurements in (A) HEKS101 cells, n=72, (B) Jurkat T cells, n=244, and (C) effector Th cells, n=102. 500 μM of H₂O₂ (arrow) was added following CRAC channel activation by 1 μM Tg. (D) I_{CRAC} in Jurkat T cells was induced by store depletion with 10 mM EGTA and analyzed at -80 mV (representative experiment is shown). 500 μM H₂O₂ was added at ~ 3 min (arrow). Current-voltage relationship (E) and average CD ± SD (F) at 300 s of untreated cells (black, n=5) or of cells treated for ~120 seconds with 500 μM H₂O₂ (red, n=6) following I_{CRAC} development.

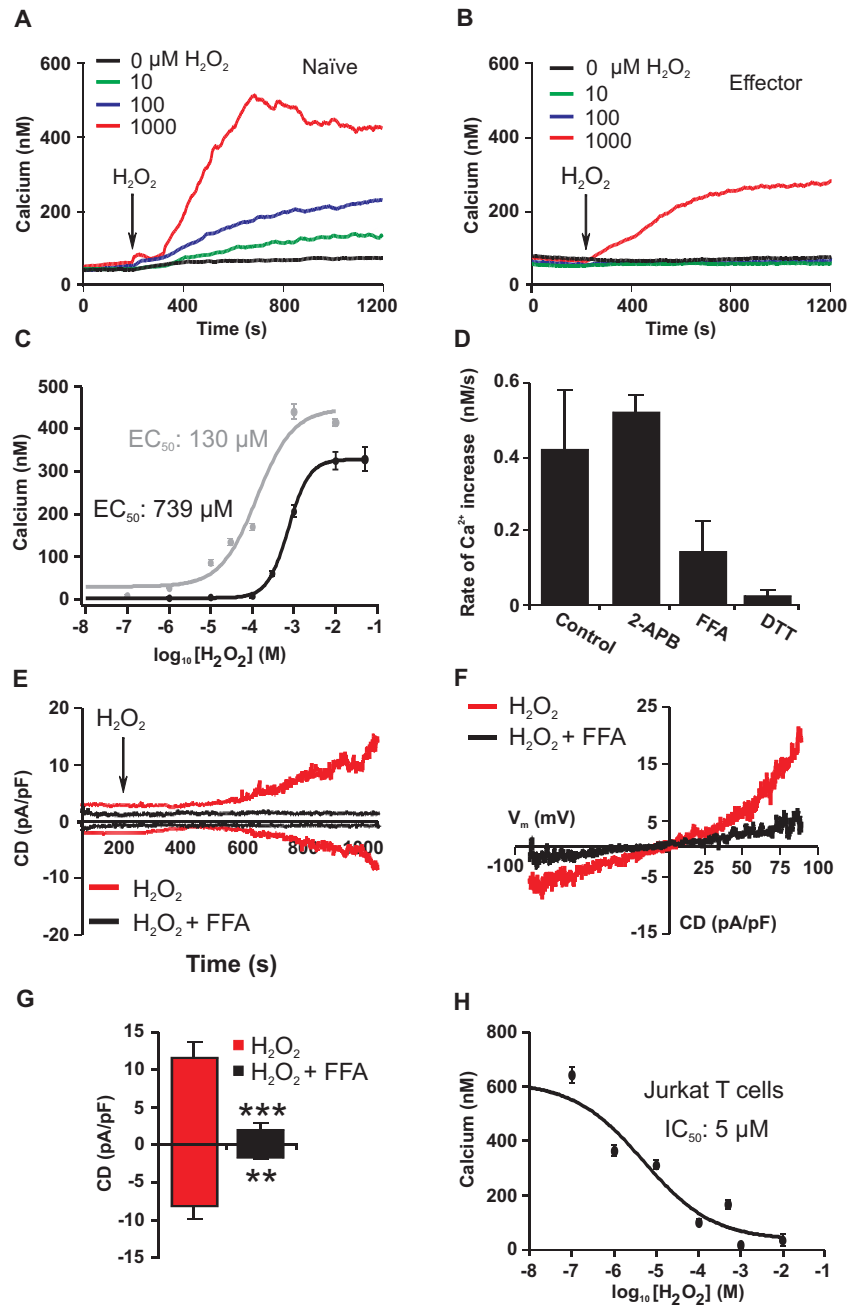


Figure S3: H₂O₂ activates nonselective ion channels.

(A, B) [Ca²⁺]_i in naïve (A) and effector Th cells (B). H₂O₂ was added as indicated. n = 340 (A) and 239 (B) for all conditions. (C) Dose dependence of [Ca²⁺]_i on [H₂O₂] ([Ca²⁺]_i @ 1190 sec - [Ca²⁺]_i @ 190 sec) ± SEM. Naïve Th cells (grey), effector Th cells (black). (D) The effect of 100 μM 2-APB, 100 μM FFA and 10 mM DTT on H₂O₂ (500 μM) induced increase in [Ca²⁺]_i. Slope calculations (nM against time) were used to determine the rate of increase in [Ca²⁺]_i induced by H₂O₂. Data are mean ± SD (n=3). (E) H₂O₂-induced current measurements in Jurkat T cells. Currents were analyzed at -80 mV and at +80 mV ramp potential and plotted against time: red (1 mM H₂O₂), black (1 mM H₂O₂ + 100 μM FFA). (F) Current-voltage relationship of cells treated with 1 mM H₂O₂ (red, n=5) and cells treated with 1 mM H₂O₂ and 100 μM FFA (black, n=4). (G) Average CD ± SD after 800 s. (H) Dependence of [Ca²⁺]_i on [H₂O₂] ([Ca²⁺]_i @ 2000 s - [Ca²⁺]_i @ 1200 s) ± SEM in Jurkat T cells.

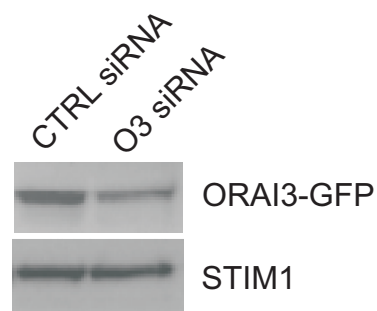


Figure S4. *Orai3* siRNA downregulates ORAI3 protein. HEK293T cells were transiently transfected with 1 μ g ORAI3-GFP and either 1.6 μ M CTRL siRNA or with 1.6 μ M O3 siRNA. Cells were lysed after 48 h. Detection using anti-GFP or anti-STIM1 antibodies.

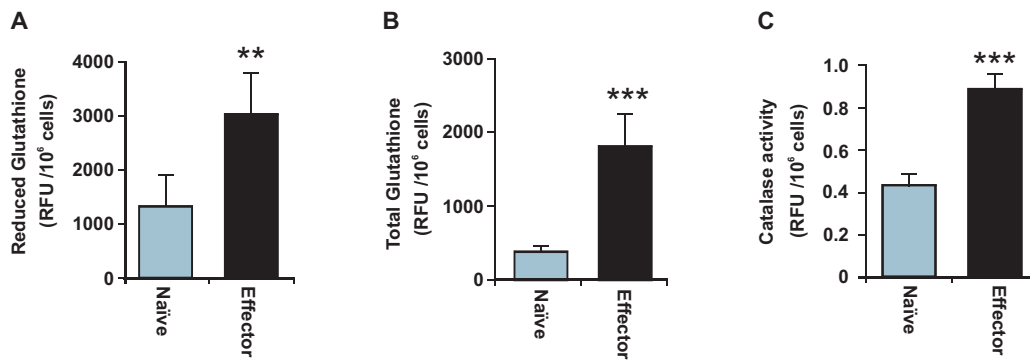


Figure S5: Relative amounts and activity of cellular antioxidants in naïve and effector Th cells.

Reduced (A) and total (B) glutathione concentration in naïve (light blue, n=5) and effector (black, n=5) Th cells. Data are mean \pm SD. (C) Catalase activity in naïve (light blue, n=7) and effector (black, n=6) Th cells. Data are mean \pm SD.